

Statistical Modeling Cement Heat of Hydration

Paul Stutzman¹ Stutz@nist.gov 301-975-6715, (corresponding author)

Stefan Leigh²

Kendall Dolly²

Abstract

The heat of hydration of hydraulic cements results from the complex sets of phase dissolution and precipitation activity accompanying the addition of water to a cement. Heat of hydration is currently measured in one of two ways: 1) through an acid dissolution of the raw cement and a hydrated cement after seven days, or 2) isothermal calorimetry. In principal, the heat of hydration should be predictable from knowledge of the cement composition, and perhaps some measure of the cement fineness or total surface area. The improved mineralogical estimates provided by quantitative X-ray powder diffraction, together with improved statistical data exploration techniques that examine nonlinear combinations of candidate model constituents, are used to explore alternative predictive models for 7-day heat of hydration (HOH₇). An All Possible Alternating Conditional Expectations (APACE) exploratory tool, created by combining All Possible Subsets Regression with Alternating Conditional Expectation (ACE), is used to determine which variables *within* an explanatory variable class and which subsets of variables *across* explanatory variable classes exhibit the highest potential predictive power for additive nonlinear models for HOH₇. While a single, strong model for HOH₇ did not emerge from these analyses, some general conclusions did result. Good fitting models include a key structural mineralogical phase (belite preferred), a calcium sulfate phase (bassanite preferred), a total fineness or surface area component (Blaine fineness preferred), and ferrite in conjunction with Fe₂O₃, or aluminate, or cubic aluminate.

¹ Materials and Construction Laboratory, National Institute of Standards and Technology
Gaithersburg, Maryland 20899-8615

² Statistical Engineering Division, National Institute of Standards and Technology
Gaithersburg, Maryland 20899-8615

Introduction

Hydraulic cements react with water through a process called hydration via a series of chemical reactions, ultimately resulting in the precipitation of interlocking hydration products that provide strength to the structure. The hydration process produces heat that in some concrete placements may cause expansion and, potentially, cracking upon cooling to ambient conditions. The temperature rise can also be beneficial in the case of cold-weather concrete placements, where the heat facilitates hydration and keeps the concrete from freezing [1].

ASTM C186, adopted in 1944 as a standard test method for determining the heat of hydration of hydraulic cements, involves measurement of the heat of solution of dry cement specimens that have been hydrated for 7 d and for 28 d. The difference between the heat of solution values between the dry and the partially hydrated cement specimens is taken as the heat of hydration for that time period. The heat values range from 261 kJ kg^{-1} to 468 kJ kg^{-1} , expressed in SI units³. This test is time-consuming, involves a hazardous mixture of nitric and hydrofluoric acids, and has low precision with the 95 % limits on the difference between two test results (d2s) values of 48 kJ kg^{-1} for measurements between different laboratories. Conduction calorimetry provides an alternative with ASTM C1679, “Standard Practice for Measuring Hydration Kinetics of Hydraulic Cementitious Mixtures Using Isothermal Calorimetry”. This method has been shown to be useful in the estimation of total heat, in assessing early-age reactions and setting problems, and in measuring the influences of sulfate additions and mineral admixtures on heat evolution [2].

The rate of hydration of a cement depends upon its mineralogy, the mass fraction of each phase, the particle size distribution, the water-to-cement ratio, and the temperature and relative humidity of curing [3]. Copeland et al. [4] ascribe the total heat of hydration as emanating from two processes: 1) the chemical reactions in the formation of hydration products, thought to be responsible for 80 % of the heat, and 2) the heat of wetting of the subsequent colloidal hydration product accounting for the remaining 20 %. The C186 test utilizes a fixed water/cement ratio but the curing temperature may differ depending upon the rate of heat evolution.

Limits on composition and fineness in ASTM C150 and AASHTO M85 reflect their influences on the heat of hydration. Type II cement with the moderate heat option has two alternative restrictions on either the sum of mass % $C_3S + 4.75 * C_3A \leq 100$ (the heat index equation), or a seven-day heat release amount of 290 kJ kg^{-1} when measured by ASTM C186. Type IV (low heat cement) has limits on either phase mass fraction for C_3S , C_2S , and C_3A of 35 %, 40 %, and 7 %, respectively, or a C186 heat value limit of 250 kJ kg^{-1} at seven days. Type III cements generally have higher heats of hydration and Type IV the lowest [1].

These phase estimates are Bogue-calculated values as described in ASTM C150 and AASHTO M85. Errors in these estimates arise from the variability of clinker phase chemistry relative to the assumed compositions, from the failure to account for minor constituents, and from inaccuracy in measured analytical values [5,3]. Phase abundance directly determined by

³ Non-SI units (cal/g) may be converted by multiplying by the conversion factor 4.1868.

quantitative X-ray powder diffraction analysis (XRD) and some non-phase variables (particle size distribution, fineness) considered to affect heat evolution are considered in this work in modeling 7-day heat of hydration (HOH₇). A standard test method for clinker and cement XRD may be found with ASTM C1365 [6]. XRD is ideally suited for fine-grained materials (like clinker and cements) for direct phase analysis, as each phase produces a unique diffraction pattern independent of the other phases, the intensity of which is proportional to its concentration [7,8,9].

Effects of Cement Phase Characteristics

Early work on developing predictive models for heat of hydration focused on the contributions of the individual clinker phases, the synergistic effects of multi-phase cement hydration, and the heat of precipitation of the resulting hydration products [4,10,11,12]. Lerch [13] concluded that gypsum retards early hydration of cements that have high tricalcium aluminate content, while accelerating hydration of cements with low tricalcium aluminate content, and that the alkali aluminate (the orthorhombic form) is more reactive and requires a larger gypsum addition than a low-alkali aluminate (the cubic form). More recently, the accelerating effects of potassium oxide (presumably from the alkali sulfates and alkali-substituted tricalcium aluminate) on alite, ferrite, and aluminate have been demonstrated [14,15,3]. Calcium sulfate additions have an accelerating effect on hydration of the silicates and ferrite while retarding the initial set and the reactions of the aluminate phases. Gypsum has also been seen to retard heat development in mixtures of clinker phases. In cases where gypsum may have been partially dehydrated during cement processing forming bassanite (hemihydrate), heat (192 kJ kg⁻¹) would evolve upon rehydration to gypsum [10,11]. Overall, this reflects the complex synergy of the mineral constituents of the portland cement system during the hydration process. Confounding this further is the influence of mineral surface areas exposed upon grinding and the potential change in some mineral forms upon grinding.

Taylor [3] summarized multilinear predictive models of the form of eqn. 1 for heat (H_t) derived by least-squares regression analyses using Bogue potential phase mass fraction (μ), and a coefficient accounting for degree of hydration of each phase for a specific age (Table 1). Note that the aluminate (C₃A) reaction can result in ettringite (AFt) at early ages and monosulfate (AFm) at later ages, with differing enthalpy of hydration, underscoring the complexity of the cement hydration process. Taylor [3] notes that the enthalpies of formation of clinker phase hydration products would refine estimates of potential heat evolution, but the uncertainties in their values and variability in the reaction stoichiometry of hydration would also introduce additional errors into the estimates.

$$H_t = a \cdot \mu_{C_3S} + b \cdot \mu_{C_2S} + c \cdot \mu_{C_3A} + d \cdot \mu_{C_4AF} \quad \text{Eqn. 1}$$

Poole summarized work relating Bogue phase composition to heat of hydration and developed a multilinear regression model (eqn. 2) that utilized aluminate and alite with an R² of 89 % on the data used to develop the model, exhibiting apparently little bias, and a ± 21 kJ kg⁻¹ 95 % confidence interval on the regression [16]. The cement fineness, as measured by Blaine permeability, was not found to be a significant variable.

$$\text{HOH}_7 (\text{kJ kg}^{-1}) = 133.9 + 9.36 \cdot \mu_{\text{C}_3\text{A}} + 2.13 \cdot \mu_{\text{C}_3\text{S}} \quad \text{Eqn. 2}$$

Phases not included in these predictive models, like the alkali and calcium sulfates and the different forms of tricalcium aluminate, can exert significant influences on a cement's hydration characteristics. It is reasonable to ask whether a more complete accounting for cement phases and fineness measures will provide a better set of predictive variables. More generally, would one expect relatively simple multilinear models to work well given the complexity of hydration processes?

The Data

The variables analyzed in this work are organized into logical groupings as shown in Table 2. Data were collected for 22 cements from the CCRL proficiency test program, 18 cements from a NCHRP program 18-05 on cement performance [17], and 4 cements provided by the US Army Corps of Engineers. The QXRD data were the average of three replicates each of a bulk cement and an extraction residue after a salicylic acid / methanol extraction to facilitate identification and quantitative estimates. Bulk oxide and Bogue-calculated values were used for comparative purposes and setting times and 3-day strength were selected as they had been mentioned in studies as being relevant [3].

Fineness Measures

All other variables held equal, a more finely ground cement might be expected to react more rapidly than a coarser cement. However, this does not always seem to be the case in actual practice. The Blaine fineness is an indirect measure of total particle surface area, denominated by volume of material, based on time for unit volume air to flow through a cement powder packed cylinder [18]. An alternate means of measuring cement fineness is through particle size distribution. Laser diffraction of cements provides size distribution data using measures of D10, D50, and D90, indirect measures of 10th/50th/90th percentiles of particle size distribution. Span, an additional variable is a function of these three, measuring the approximate range of the particle size distribution.

Time of Setting

The Vicat test measures the penetration depth of a standardized needle, where initial and final set times are when the needle penetrates a cement paste less than prescribed limits of 25 mm and zero mm, respectively [19]. Since it is the difference between the final and initial times, (VicatF - VicatI), which is the true test correlative with speed of setting, HOH₇ may be expected to correlate with [1/(VicatF - VicatI)]. This simple example illustrates the occasional need to transform raw variables in order to achieve meaningful variable response. A potential confounding factor with this test procedure is the use of normal consistency paste, where the prescribed water content for the Vicat test will vary by cement, which may affect the setting times, and may be different from the HOH test conditions.

Statistical Modeling

Historically, modeling responses like HOH₇ typically have involved multilinear modeling of raw (test data) inputs or judiciously transformed inputs, with transformations motivated by established engineering relationships. Examples of this are the multilinear Bogue models relating oxide compositions to mineralogical phase compositions. Typically the existing models have been derived by straightforward multilinear fitting, or by forwards or backwards selection techniques that progress in an automated fashion through choices of subsets of potential predictor variables, comparing explanatory power gained by successive addition or deletion of variables through reductions or decreases in R², or residual variance, or F statistic. Over the last forty years, however, sophistication in model selection techniques for both multilinear candidate models and interesting nonlinear extensions of multilinear models has increased tremendously.

In our initial approach to modeling HOH₇ based on the mineralogical, fineness, and particle size distribution data, we employed All Possible Subsets Regression (APSR) [20] and a nonlinear-addend multilinear fits obtained by the use of Alternating Conditional Expectation (ACE) [21]. While these techniques are not new, using them separately and in conjunction offers significant improvements over backwards / forwards selection techniques.

Our key tool, though, was All Possible Alternating Conditional Expectations (APSACE) created by combining the All Possible Subsets Regression, APSR, with Alternating Conditional Expectation, ACE. Using APSACE, we can easily explore which variables *within* an explanatory variable class and which subsets of variables *across* explanatory variable classes exhibit the highest potential predictive power for additive nonlinear models for HOH₇. An additive nonlinear model is a weighted sum of nonlinear function summands. We find APSACE linked with the use of automated parametric fitting tools^{4,5} to be an easy-to-use, easy-to-interpret, and insightful approach to meaningful model search that offers an enormous extension of the classical automated model search employing only multilinear functions.

Since our algorithm assays combinations by exhaustion, we limit ourselves to combinations of less than or equal to 10 variables. But for the size of the dataset being examined, and the number of explanatory variables being considered, that does not appear to be unduly restrictive. Nonetheless, since a number of the basic techniques used in developing and selecting multilinear models are still applicable, in practice or at least in motivating more modern approaches, we spend a little time discussing APSR and associated statistics.

Prescreening Variables: Scatterplots

A fundamental principle of modern exploratory data analysis, including model selection, is to prescreen data. Graphical prescreening enables the modeler to (1) scan for outlying data or obviously anomalous patterns in data, (2) to gauge the potential statistical explanatory power and

⁴ Certain commercial materials and equipment are identified to adequately specify experimental procedures. In no case does such identification imply recommendation or endorsement by the National Institute of Standards and Technology, nor does it imply that the items identified are necessarily the best available for the purpose.

⁵ TableCurve 2D, <http://www.sigmaplot.com/products/tablecurve2d/tablecurve2d.php>

potential model meaningfulness of each explanatory variable assessed against the response [variable] of interest (HOH7).

A cross-correlation table of the variables serves another purpose. Variables that cross-correlate highly may contain much the same explanatory information for the proposed model. Incorporating both in a model may lead to either an unnecessary degree of redundancy, or over fitting, in the model or to numerical instabilities (e.g., multicollinearities) in the numerical fitting procedure. Alite and belite (variables C₃S and C₂S, respectively) are highly anticorrelated. This is a natural result of their physical co-occurrence as calcium silicates at the expense of one another. The natural modeling solution is to employ one or the other, selecting the variable for the model situation that gives the best goodness-of-fit statistics.

All Possible Subsets Regression (APSR)

All Possible Subsets Regression regresses a response variable (HOH7) against all possible multilinear combinations of a pre-selected set of explanatory variables, typically screening for the best model fits from among the many fitted using criteria such as R² and exhibiting only the best models fit as judged by the goodness-of-fit criteria. In standard software⁶, the many regressions performed in APSR are multilinear regressions with up to 32 input variables. While it is a linear tool, it is still an excellent screening device, and to be preferred to forward or backwards model subset selection.

So, for example, if there are 10 candidate explanatory variables, APSR software performs

$$(2^{10} - 1) = {}_{10}C_1 + {}_{10}C_2 + \dots + {}_{10}C_{10} \quad \text{Eqn. 3}$$

or 1,023 regressions, where " ${}_{10}C_1$ " means all possible 1-variable-at-a-time models, " ${}_{10}C_2$ " means all possible 2-variable-at-a-time-combination models, and so forth. Goodness-of-fit is typically assessed by Residual Sum of Squares (RSS).

$$RSS = \sum_{\text{all data}} \frac{[HOH7 - Model Prediction]^2}{(N - P)} \quad \text{Eqn. 4}$$

where the sum is taken over all the data points, N is the number of data points, P is the number of parameters being fitted (typically either number of explanatory variables or number of explanatory variables + 1 if an additive constant is being fitted as well). Since an RSS of zero denotes a perfect error-less fit, the closer to zero the RSS from a real data fit the better [22].

The Coefficient of Determination, or R²,

$$R^2 = \frac{\sum (pred(HOH7) - mean(HOH7))^2}{\sum (HOH7 - mean(HOH7))^2} \quad \text{Eqn. 5}$$

⁶ BMDP: <http://www.statistical-solutions-software.com/products-page/bmdp-statistical-software/>

quantifies the improvement of the model-under-investigation's predictive performance over the naive mean model's (the most primitive model) prediction. It is often referred to as quantifying the percent of variation in the data explained by the model; the statistic is multiplied by 100 to express it in percent. Expressed in that way, it is clear that the closer the value of the R^2 to 1, or 100, the better as a value of 1 or 100 connotes a perfect fit.

Misspecification: Model Bias

In comparing candidate models' performance, it is not enough to restrict attention to goodness-of-fit statistics. Because, in general, the more variables (parameters) one adds to a model, the better the fit will be. There is also the issue of protecting against model misspecification, or model bias, referring to the possible inclusion of too few or too many predictor variables in the model. For example, on any given pass of an all possible subsets routine if variables are being included that shouldn't be in the model, the variances (noise levels) of model coefficients and predictions increased and pushes predictions off target. On the other hand, if too few variables are being included in the model, the model will be biased and predictions pushed off target.

Since simply increasing the number of variables incorporated in a model will automatically tend to improve such goodness-of-fit statistics, reference must also be made to an adjustment for bias statistic such as Mallows's C_p , where the "bias" in question refers to the biasing of a model by the incorporation of too few or too many explanatory variables

Mallow's C_p

Mallow's C_p statistic is very useful for assessing misspecifications when comparing multilinear models. It assesses the balance between bias due to too-few variable and too-many variables by evaluating

$$C_p = \left[\frac{\sum(\text{VAR}(\text{predHOH7}))}{\sigma^2} \right] + \left[\frac{\sum(\text{BIAS}(\text{predHOH7}))}{\sigma^2} \right]$$

$$= p + \frac{\left(s^2 - \hat{\sigma}^2 \right) \cdot (n - p)}{\hat{\sigma}^2} \quad \text{Eqn. 5}$$

where p is the number of parameters in the candidate model, s^2 is the residual mean square for the candidate model, and $\hat{\sigma}^2$ is an estimate of the true model variance.

A C_p value close to p indicates minimal misspecification in a candidate model. The use of C_p in conjunction with a goodness-of-fit metric like R^2 is probably the single most reliable

approach to "fitting blind", i.e. searching by statistical trial-and-error for a model where no scientifically derived candidate model exists [23,24,25].

Ensuring Model Validity

To ensure model validity generally, one seeks a number of objectives:

1. physical meaningfulness: use of scientifically meaningful variables in the model,
2. goodness-of-fit: in the RSS or R^2 metric,
3. parsimony: employing as few variables as possible in the model without overly under-fitting and without sacrificing too much goodness-of-fit,
4. avoiding misspecification,
5. cross validation: testing the goodness-of-model achieved on a set of training data by cross-validating against a non-training set (not performed in this study).

APSR Analysis

In this work, we subjected various combinations of the chief untransformed variable classes to APSR analysis. The results of the best for each combination are summarized in Table 3. From these combinations, key variables were selected, generating grouping 7 in Table 3, noted as the "best of best" and reflecting the comparatively high R^2 and C_p statistic close to the number of variables. It is interesting to note that the combination of alite and aluminate that form the basis for the ASTM and AASHTO heat index equation does not appear in this table, although alite in combination with other phases, fineness measures, and oxides does. The results suggest that Blaine fineness may be the best predictor from among the fineness variables considered. While the R^2 values are not strong for these models, they serve to indicate potentially interesting candidate variables for the subsequent step of nonlinear transformation of the data.

In each instance of class combination, the combination with the best statistics is reported. In categories where the mineral variables were included (five of seven), some form of calcium sulfate is selected as a key variable, specifically bassanite and/or anhydrite. The Fe_2O_3 and TiO_2 significance may lie in their occurrence primarily in the ferrite phase, and to a lesser extent co-occurrence with the aluminates and belite [3]. When the particle size distribution variables are included among the candidate predictor variables, most often the Blaine fineness is chosen. Interestingly, TiO_2 recurs frequently in conjunction with Fe_2O_3 and ferrite in good models. We will see this again when we explore nonlinear transformations with APSACE-selected models with $R^2 > 0.90$.

Alternating Conditional Expectation

Alternating Conditional Expectation (ACE) is a technique that greatly extends the scope of classical multilinear model selection techniques [26]. Given HOH_7 data with associated candidate predictor variables X_k , the ACE algorithm finds transformations of the predictor variables and of the HOH_7 response variable that maximize the correlation between $f(HOH_7)$, the

transformed HOH_7 , and $\sum g_k(X_k)$, the sum of the transformed predictor variables. The transformations are produced nonparametrically in the forms of pictures [28], relating transformed to original variable for each of the variables, including HOH_7 response. Such pictures can be parametrically modeled either from first principles or by the use of automated software. As the transformation graphs can assume many forms, they need to be evaluated for credibility for incorporation into the predictive model. Analyzing each transformation picture for smoothness performs this evaluation. Transforms that would appear to be approximately straight lines, low order polynomials, exponential or logarithmic functions, or circular functions are candidates for incorporation in a model. Transforms with severe inflection points or that have the appearance of multiple distinct behaviors adjoined, for example, might not be considered candidates for incorporation in the model, or might be modeled distinctly for each simple sub-model regime.

In using the ACE algorithm, one notices very quickly that ACE drives R^2 up dramatically. If one feeds 7 or 8 candidate explanatory variables into a model of HOH_7 , one can easily obtain R^2 values on the order of 0.80 to 0.95, possibly irrespective of how meaningful the incorporated variables are for the "true" prediction of HOH_7 . Some of the transformations will look smooth and easily parameterizable, but some will not. Since re-ACE-ing subsets of variables can give different transformations from ACE-ing the original full set, it is clear that the appropriate way to proceed for optimal variable selection purposes is to perform an All Possible Subsets ACE (APSACE) of the original full set of variables. That is, match HOH_7 response to one variable at a time, then two variables at a time, then three variables at a time, etc., ACE-ing each distinct combination. That is what we have done, using a nested loop of S-plus code⁷ [27,28]. Doing this guarantees that the ACE transform outputs for each distinct combination of variables is mathematically meaningful and complete. For future work, one might consider augmenting the APSACE statistics with a C_p analog and then outputting only the highest R^2 with C_p closest to p combinations. In doing so, however, one might easily ignore interesting subsets of variables that are consistent contributors to good models and that consistently transform cleanly.

Explicit Parameterization of ACE outputs: an example

Running APSACE on a candidate predictor set that includes aluminate, ferrite, bassanite, Blaine, and $1/\text{Vicat}$ yields four different high- R^2 subclusters (Table 4). It is interesting that the ACE transform for $1/\text{Vicat}$ is close to linear for all subclusters until bassanite is added. This is an example of the kind of persistence of inclusion in high R^2 models coupled with persistence of transformation shape that might signal the importance of a variable. Why might a model incorporating these variables be good? Blaine fineness is an indirect measure of the total particle surface area, which should affect the rate of heat release. Ferrite occurs as medium- to fine-grained crystals that should exhibit greater surface area than some of the other "structural" mineral phases and its enthalpy of complete hydration ranks just below that of alite. Additionally, at 7 days, the reaction coefficient is almost twice that of alite (Table 1). And, as explained above, high HOH_7 may also promote a rapid setting time, associated with a low Vicat.

⁷ <http://spotfire.tibco.com/products/s-plus/statistical-analysis-software.aspx>

For illustration purposes only, we show how using automated software can parameterize one of the APSACE-suggested models of Table 10. The second example from Table 10 combines relatively smooth or linear transforms with a relatively high R^2 (0.88), the plots of each transformed variable being shown in Figure 1. From a large menu of potential parametric fits to any given ACE transform, we generally select the model that seems to give the best combination of high R^2 , visual goodness-of-fit, and is parsimonious in the number of parameters used in the parameterization.

If ACE (HOH₇) can be modeled, either as a simple linear function (which in practice it is often) or more generally as an explicitly invertible function (e.g., log-to-exp or sin-to-arcsin), we obtain a completely explicitly parameterized model for HOH₇ in terms of ferrite, bassanite, and (1/Vicat). The three-variable ACE model developed here, without the explicit parameterization, gives an R^2 on the data modeled of 0.88. The two-variable Poole model in Eqn. 2 gives an $R^2 = 0.76$ [16]. However, the model considered here for illustrative purposes only, is just one among dozens of high- R^2 ($R^2 > 0.90$) candidate models that APSACE has identified.

As illustrated in Figures 2 - 4, a simplified cubic fit coarsely captures the main structure in the ferrite transform, a $x-(1/x)$ quadratic captures Blaine structure, and a line captures some of the descent of the (1/Vicat) transform. It should be clear that approximate parametric fitting of each ACE transformation will contribute to a diminution of the overall model fit's R^2 (0.88), as each approximate parametric fit reduces that variable's contribution to R^2 .

Substituting the best-fit parameterizations into the APSACE candidate model gives

$$\begin{aligned} ACE(HOH_7) &= ACE(F) + ACE(B) + ACE(V) \\ &= (0.06 + 0.009F^2 - 0.0007F^3) + \left(535 - 0.12B + (9 \cdot 10^{-6})B^2 - \frac{773336}{B} \right) + (-120V + 1.3) \end{aligned}$$

where

- F = ferrite
- V = 1/Vicat
- B = Blaine

If ACE(HOH₇) were easily parametrically invertible (approximately a straight line), the application of the inverse of ACE(HOH₇) to the right hand side of the equation would yield a parametric equation for HOH₇ in terms of ferrite, Blaine, and inverse Vicat. In this example, however, the ACE transform of HOH₇ is sufficiently scattered that a simply invertible parameterization is unavailable.

Summary

This work has not resulted in a simple parametric model for HOH₇. Instead, we have found simple conclusions concerning the variables and the data considered that offer general guidance on the modeling of HOH₇. It is to be strongly emphasized that the one explicitly parameterized model presented is meant to be illustrative of the power of the technology only.

Good fitting models for HOH₇ often incorporate a number of attributes:

1. A structural mineralogical phase component (belite preferred);
2. A sulfate phase component (bassanite preferred);
3. A total fineness or particle surface area component (Blaine preferred);
4. Ferrite in conjunction with Fe₂O₃, and possibly TiO₂ or aluminate or C₃Ac, but not C₃Ao

The prevalence of noisy and multi-structured ACE plots in this study can possibly be attributed to multiple potential causes:

1. The inclusion of all cement Types in the dataset is inappropriate. In the future, attention should be focused for this kind of modeling on one specific Type of cement, representing possibly different heat evolution mechanisms.
2. The occasionally sharp transition, or inflection, points in the ACE plots could correspond to transition points in the variable being ACE transformed from a range of values characteristic of one Type of cement to a range of values characteristic of another Type. The break in the Blaine transform curve that consistently occurs is at a value that roughly corresponds to the differences between Type III (mean Blaine of 556 m²/kg) and Types I, II, and V (roughly 380 m²/kg) suggests that these should be modeled separately.
3. The variables are inappropriate: variables are included that have no true HOH modeling content, and variables which should be included, like precipitation products known to influence heat evolution, are not.

Acknowledgements

This work was sponsored by the American Association of State Highway and Transportation Officials, in cooperation with the Federal Highway Administration, and was conducted in the National Cooperative Highway Research Program, which is administered by the Transportation Research Board of the National Research Council.

TABLE 1 Heat of hydration values for clinker phases, and at 7 d and 28 d. From Taylor [3].

Compound	Coefficient	<i>Value of the coefficient (kJ kg⁻¹) for age (d)</i>		
		7 d	28 d	Enthalpy of complete hydration (kJ kg ⁻¹)
C ₃ S	a	222	126	-517 ± 13
C ₂ S	b	42	105	-262
C ₃ A	c	1556	1377	-1144; -1672 (AFm, AFt reactions)
C ₄ AF	d	494	494	-418

TABLE 2 Predictor Variables and Classes used in the exploratory data analysis.

<i>Mineral Phase by XRD (% mass fraction)</i>	<i>alite, belite, aluminite, cubic aluminite, orthorhombic aluminite, ferrite, periclase, alkali sulfates, gypsum, bassanite, anhydrite</i>
Bulk oxide content (% mass fraction)	CaO, SiO ₂ , Fe ₂ O ₃ , Al ₂ O ₃ , SO ₃ , MgO, Na ₂ O, K ₂ O, TiO ₂ , P ₂ O ₅ , ZnO, Mn ₂ O ₃
Fineness	Blaine; and particle size by laser diffraction: D10, D50, D90, Span
Extras (other physical measurements)	calcite Set time (Vicat) 3d strength

TABLE 3 APSR regression results according to the untransformed variable class combinations.

<i>Variable Class Combinations</i>	C_p	R^2	$R^2_{adj.}$
1) alite, ferrite, bassanite, Fe ₂ O ₃ , TiO ₂	5.55	.50	.45
2) alite, bassanite, span	-0.92	.32	.28
3) SiO ₂ , Fe ₂ O ₃ , MgO, SO ₃ , TiO ₂	2.95	.37	.30
4) C ₃ Ao, anhydrite, bassanite, 3d str	2.52	.42	.37
5) SiO ₂ , Fe ₂ O ₃ , MgO, SO ₃ , TiO ₂ , Blaine	3.40	.39	.31
6) bassanite, 3d strength, Blaine	3.19	.35	.31
7) alite, ferrite, anhydrite, bassanite, Blaine, Fe ₂ O ₃ , TiO ₂ (best of best)	7.44	.55	.48

TABLE 4. Small clusters of variables that provide high R^2 and smooth transformations. Individual variables and a description of the transform shape are provided.

R^2					
.78	Aluminate smooth, with edges			Blaine smooth with cusp	1/VICAT almost linear
.88		Ferrite smooth with drop-off		Blaine smooth with asymptote	1/VICAT almost linear
.90	Aluminate rough	Ferrite line with tent		Blaine smooth	1/VICAT almost linear
.86	Aluminate multi-modal	Ferrite rough	Bassanite high-low disconnect	Blaine rough	1/VICAT tent

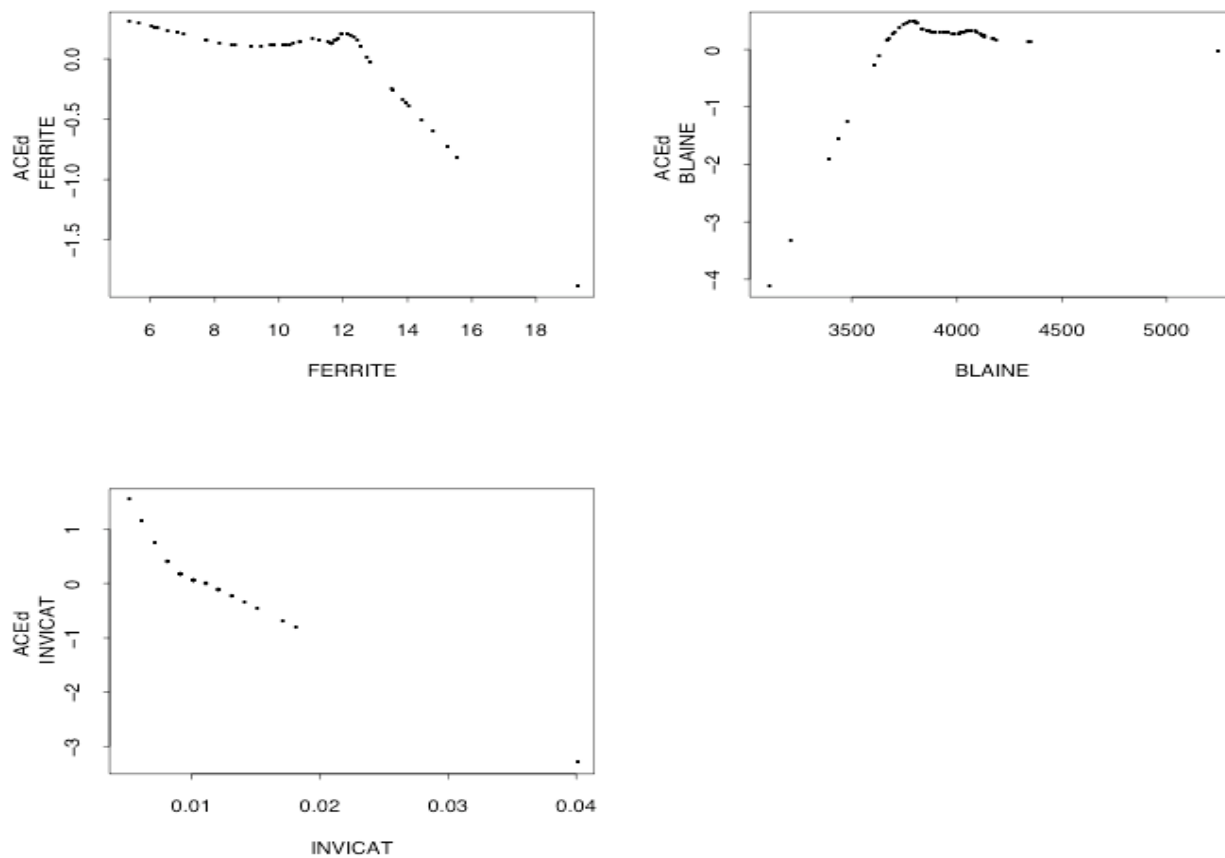


FIGURE 1 ACE transforms for ferrite, Blaine, and 1/Vicat yields a combination of a smooth transform and high R^2 of 0.88. This is the combination chosen to illustrate explicit parameterization.

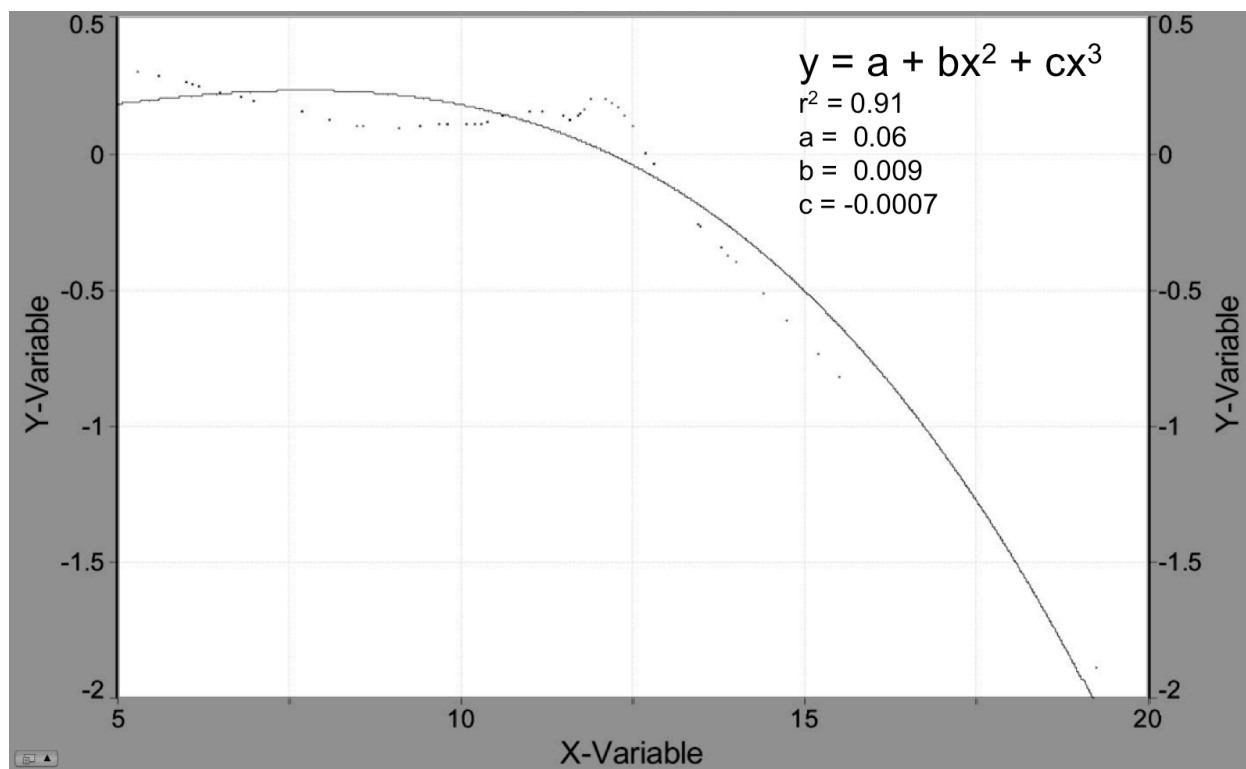


Figure 2 Ferrite ACE transform is approximately described by a simplified cubic function.

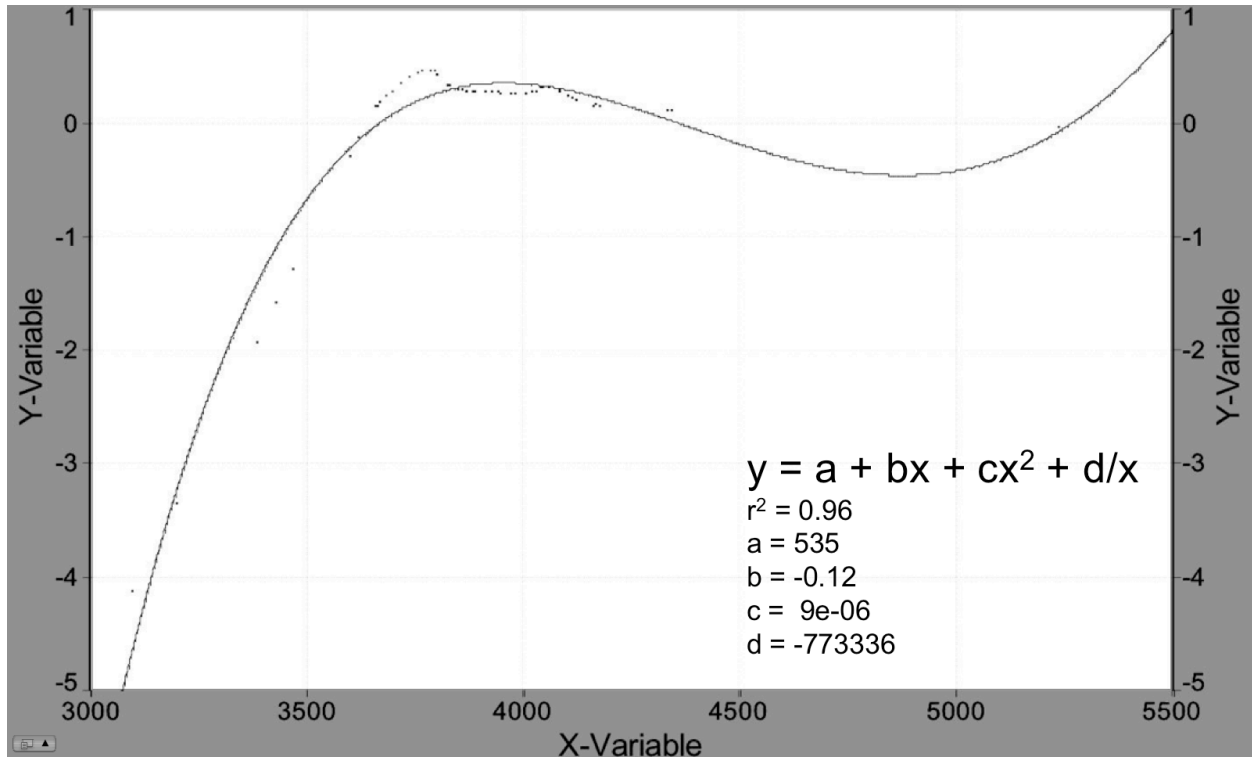


FIGURE 3 Transformed Blaine fineness can be described by a mixed $x-(1/x)$ quadratic.

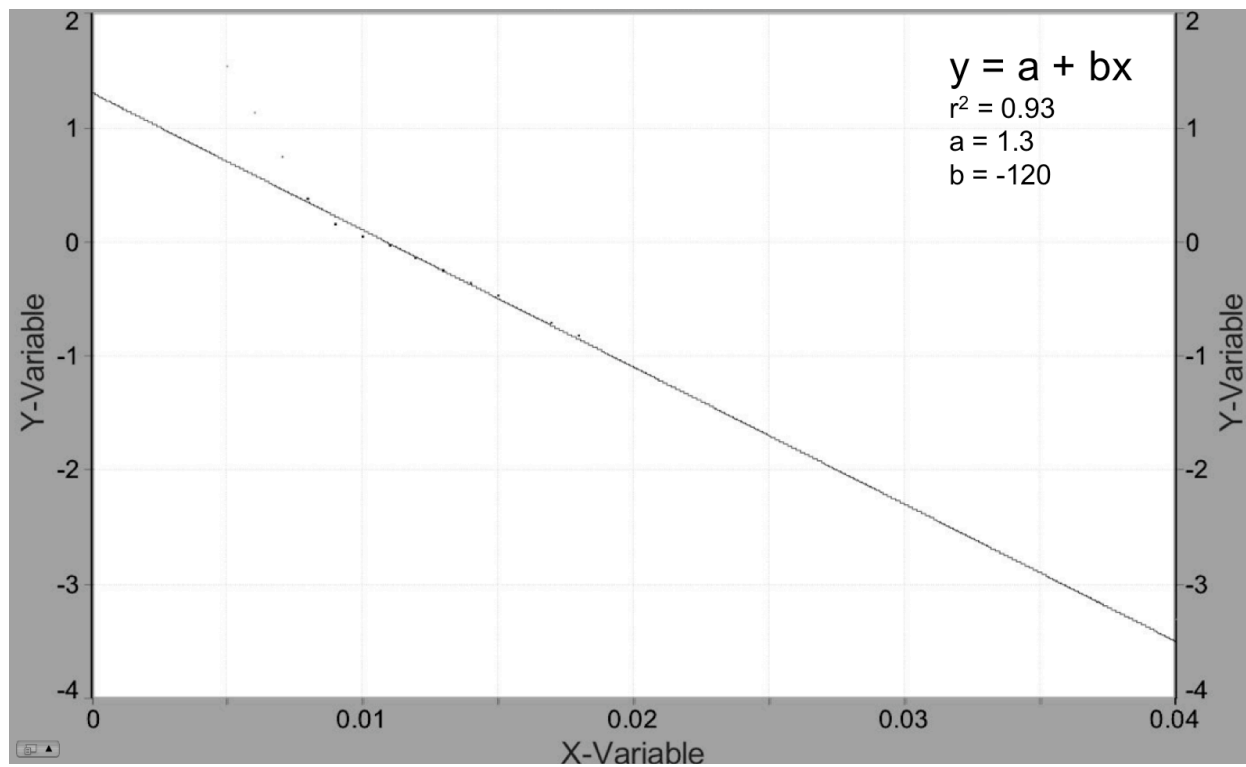


FIGURE 4 Transformed 1/Vicat results in an almost linear structure.

References

- 1 Portland Cement, Concrete, and Heat of Hydration, Concrete Technology Today, Vol. 18, No. 2, July 1997.
- 2 L. Wadsö, “Applications of an eight-channel isothermal conduction calorimeter for cement hydration studies,” Cement International, No. 5, 2005, pp. 94-101.
- 3 H.F.W. Taylor, Cement Chemistry, Thomas Telford, London, 1997
- 4 L.E. Copeland, D.L. Kantro, and G. Verbeck, “Chemistry of Hydration of Portland Cement,” Paper IV-3, pp. 429-463, Fourth International Symposium on the Chemistry of Cement, Washington, D.C., 1960
- 5 R.H. Bogue, “Calculation of the Compounds in Portland Cement”, PCA Fellowship Paper No. 21, October, 1929. Also – Industrial and Engineering Chemistry, Vol. 1, No. 4, P. 192, Oct 15, 1929.
- 6 ASTM C 1365, “Standard Test Method for Determination of the Proportion of Phases in Portland Cement and Portland-Cement Clinker Using X-ray Powder Diffraction Analysis” Annual Book of ASTM Standards, Vol. 4.01, ASTM International, West Conshohocken, PA.
- 7 P. Stutzman and S. Leigh, “Phase Analysis of Hydraulic Cements by X-Ray Powder Diffraction: Precision, Bias, and Qualification,” Journal of ASTM International, Vol. 4, No. 5, JAI Paper ID JAI101085, 11pp., 2007.
- 8 R.A. Young, ‘Introduction to the Rietveld Method’, in IUCr Monographs on Crystallography, 5, The Rietveld Method, R.A. Young, ed., pp. 1-37,
- 9 L.J. Struble, L.A. Graf, J.I. Bhatti, “X-Ray Diffraction Analysis”, in Innovations in Portland Cement Manufacturing, Chapter 8.2, J.I. Bhatti, F. M. Miller, and S.H. Kosmatka, eds, PCA SP 400.01, 2004, 1367 pp.
- 10 R.H. Bogue and Wm. Lerch, “Hydration of Portland Cement Compounds,” Portland Cement Association Fellowship at the National Bureau of Standards Paper No. 27, 30 pp., August 1934.
- 11 R.H. Bogue, The Chemistry of Portland Cement, Reinhold Publishing, New York, 1955.
- 12 L.J. Parrot and D.C. Killoh, “Prediction of Cement Hydration,” in British Ceramic Society Proceedings 35, pp. 41-54, 1984.
- 13 W. Lerch, “The Influence of Gypsum on the Hydration Properties of Portland Cement Pastes,” Proceedings of the American Society for Testing Materials, Vol. 46, 1946.
- 14 F.J. Tang and E. M. Gartner, “Influence of sulfate source on Portland Cement hydration,” Advances in Cement Research, Vol. 1, No. 2, April, 1988.
- 15 J. Gebauer and M. Kristmann, “The Influence of the composition of industrial clinker on cement and concrete properties,” World Cement Technology, 10(2), March, 1979, 46-51.
- 16 T.S. Poole, “Predicting Seven-Day Heat of Hydration of Hydraulic Cement from Standard Test Properties,” Journal of ASTM International, Vol. 6, No. 6, 10 pp., June 2009.
- 17 D.M. Roy, P. Tilkalsky, B. Sheetz, and J. Rosenberger, “Relationship of Portland Cement Characteristics to Concrete Durability,” in, Research Results Digest, NCHRP Project 18-05, National Cooperative Highway Research Program, Transportation Research Board, Washington, DC, 2002
- 18 “Standard Test Methods for Fineness of Hydraulic Cement by Air-permeability Apparatus,” ASTM C 204-07, Annual Book of ASTM Standards, Vol. 4.01
- 19 “Standard Test Methods for Time of Setting of Hydraulic Cement by Vicat Needle” ASTM C 191, Annual Book of ASTM Standards, Vol. 4.01

-
- 20 D. Wang and M. Murphy, "Estimating Optimal Transformations for Multiple Regression Using the ACE Algorithm," *Journal of Data Science* 2(2004), 329-346.
- 21 L. Breiman and J.H. Friedman, "Estimating Optimal Transformations for Multiple Regression and Correlation," *Journal of the American Statistical Association*, Vol. 80, No. 391, Sept. 1985, pp. 580-598.
- 22 W.J. Dixon, ed., *BMDP Statistical Software manual Volumes 1,2*. University of California Press, Berkeley, 1992.
- 23 R.H. Meyers, *Classical and Modern Regression with Applications*, Duxbury Press, Boston, 1986.
- 24 L.C. Hamilton, *Regression with Graphics: A Second Course in Applied Statistics*, Brooks/Cole/Wadsworth, Belmont, CA, 1992.
- 25 J. Neter, M.H. Kutner, C.J. Nachtsheim, and W. Wasserman, *Applied Linear Statistical Models*, 4th Edn., WCB/McGraw-Hill, Boston, 1996.
- 26 T.J. Hastie and R.J. Tibshirani, *Generalized Additive Models*, London: Chapman and Hall, 1990.
- 27 M.J. Crawley, *Statistical Computing: An Introduction to Data Analysis Using S-Plus*, Chichester: John Wiley, 2002.
- 28 W.N. Venables and B.D. Ripley, *Modern Applied Statistics with S-Plus*, 3rd edn. New York: Springer, 1999.